Electronic Supplementary Material (ESI) for Journal of Materials Chemistry C.

Supporting Information

Achieving halogen bonding enhanced ultra-highly efficient AIE and reversible mechanochromism properties of TPE-based luminogens: position of bromine substituents

Xinrui Miao*, Zhengkai Cai, Hengqi Zou, Jinxing Li, Songyao Zhang, Lei Ying*, and Wenli Deng

Institute of Polymer Optoelectronic Materials and Devices, State Key Laboratory of Luminescent Materials and Devices, College of Materials Science and Engineering, South China University of Technology, Guangzhou 510640, People's Republic of China.

Corresponding authors： msxrmiao@scut.edu.cn; msleiying@ scut.edu.cn

Synthesis of TBE deriatives

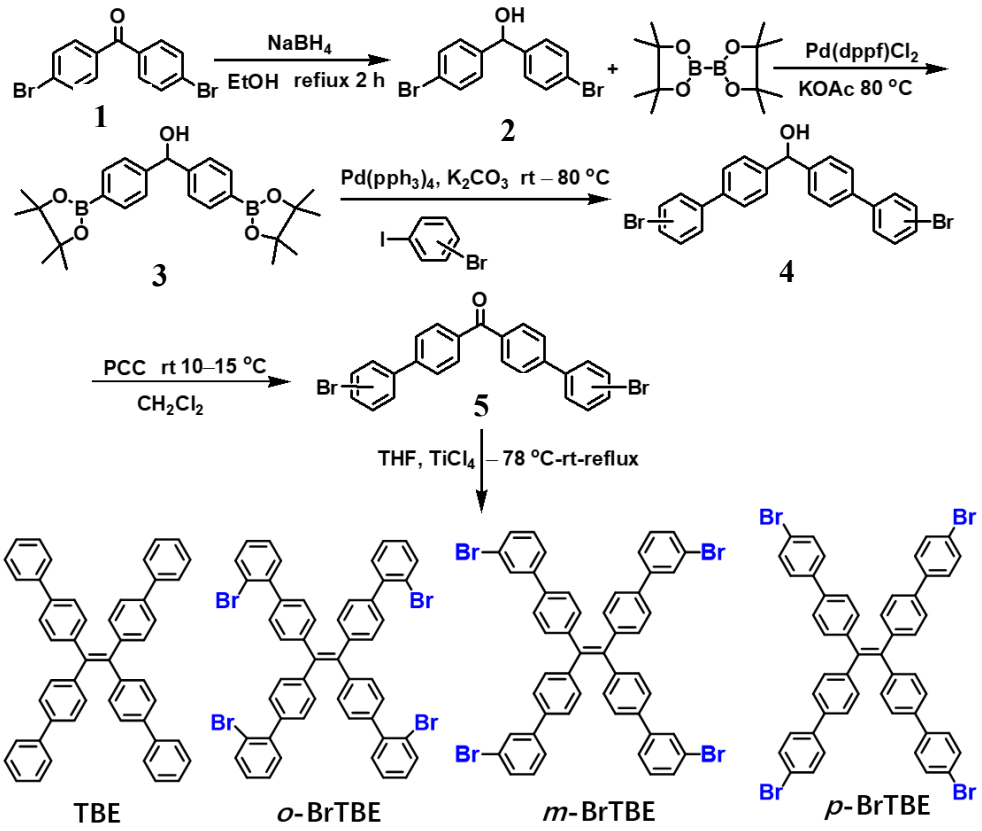

Scheme S1. Synthetic route for TBE deriatives.

The synthesis route of four compounds is similar. The synthesis and characterization of precursors, TBE, and *m*-BrTBE have been reported in our previous work.[1] Here, we provide the synthesis and characterization of *o*-BrTBE and *p*-BrTBE in the final step.

o-BrTBE or *p*-BrTBE (3.75 g, 5.0 mmol), and zinc dust (2.60 g, 40.0 mmol) were placed into a 250 mL two-necked round-bottom flask with a reflux condenser. The flask was evacuated under vacuum and flushed with dry nitrogen three times, and then dry THF (100 mL) was added. After the mixture was cooled to –78 ºC, $TiCl_4$ (3.80 g, 20.0 mmol) was then added dropwise by a syringe. After stirring for 15 min at –78 ºC, the mixture was slowly warmed to room temperature and then was heated to reflux overnight. The mixture was quenched with 10% aqueous sodium carbonate and extracted with dichloromethane three times. The combined organic layers were washed with water and dried over anhydrous magnesium sulfate. After filtration and solvent evaporation, the crude product was purified by silica gel column chromatography. Colorless solid compounds *o*-BrTBE and *p*-BrTBE were obtained in 65% and 52.9 % yield, respectively.

[1] X. Miao, Z. Cai, J. Li, L. Liu, J. Wu, B. Li, L. Ying, F. Silly, W. Deng and Y. Cao, *ChemPhotoChem* **2021**, *5, 626-631*.

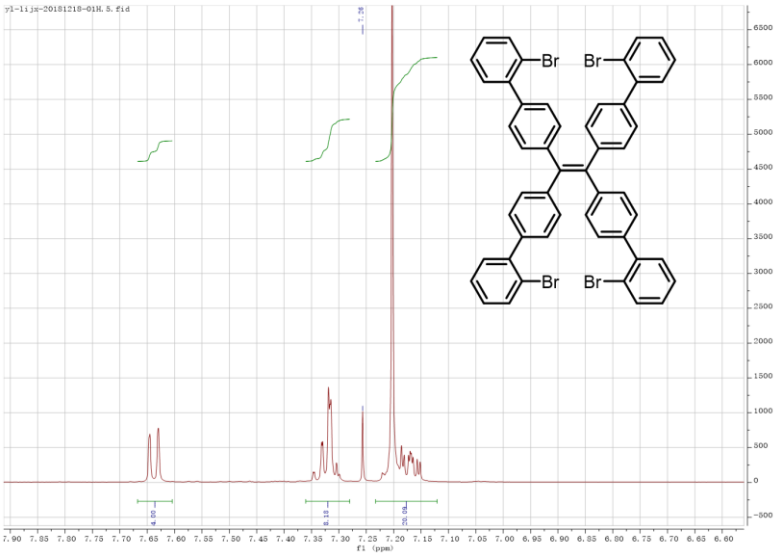

^{1}H NMR (500 MHz, Chloroform-*d*): δ 7.64 (dd, *J* = 8.0, 1.1 Hz, 4H), 7.36 – 7.28 (m, 8H), 7.23 – 7.12 (m, 20H).

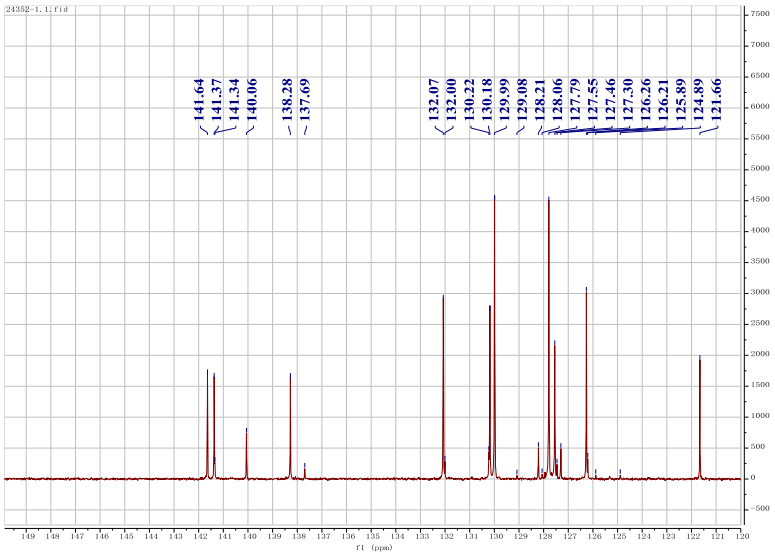

δ_C (151 MHz, $CDCl_3$) 141.64, 141.37, 141.34, 140.06, 138.28, 137.69, 132.07, 132.00, 130.22, 130.18, 129.99, 129.08, 128.21, 128.06, 127.79, 127.55, 127.46, 127.30, 126.26, 126.21, 125.89, 124.89, 121.66, 76.20, 75.99, 75.78.

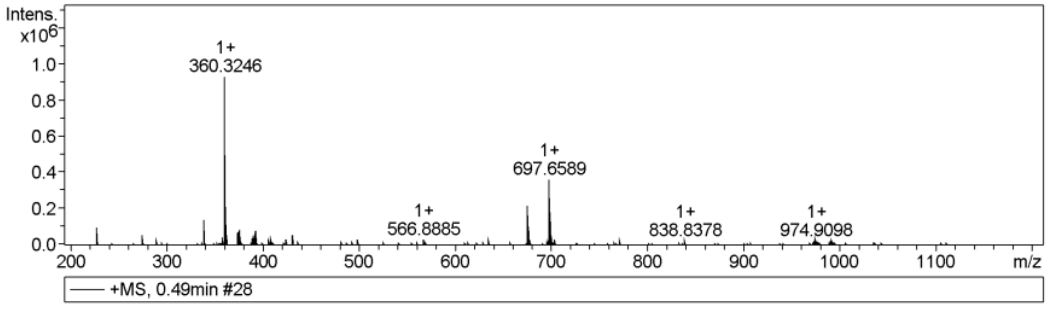

HRMS (ESI, m/z): [M]+ calcd for $C_{50}H_{32}Br_4Na$, 970.9111; found, 970.9130.

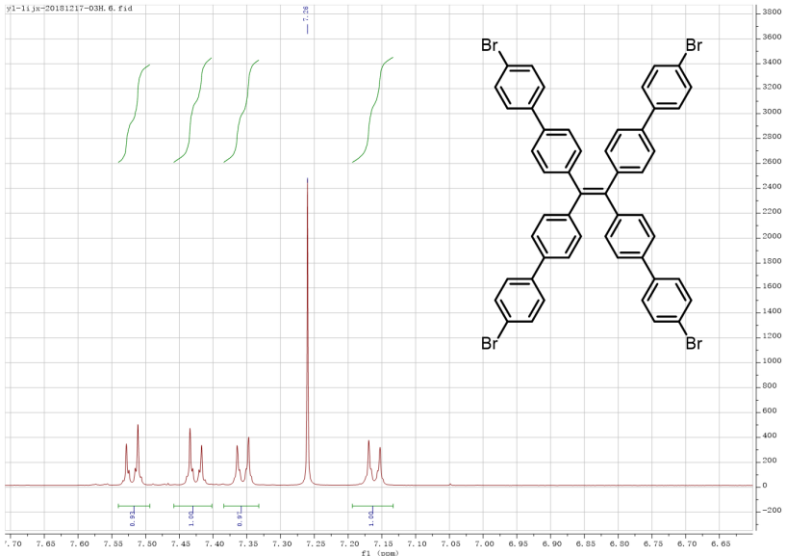

^{1}H NMR (500 MHz, Chloroform-*d*): δ 7.54 – 7.49 (m, 8H), 7.46 – 7.40 (m, 8H), 7.38 – 7.33 (m, 8H), 7.19 – 7.13 (m, 8H).

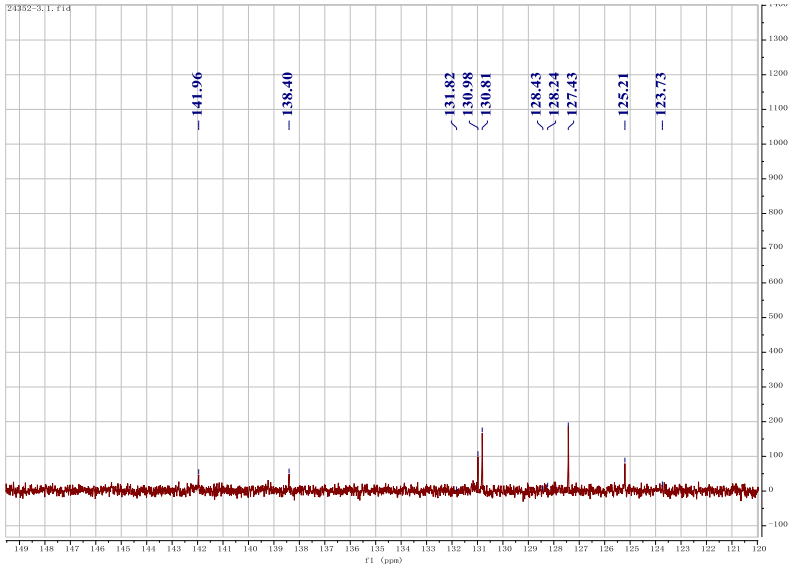

δ $_{C}$ (151 MHz, $CDCl_3$): 141.96, 138.40, 131.82, 130.98, 130.81, 128.43, 128.24, 127.43, 125.21, 123.73, 76.20, 75.99, 75.78.

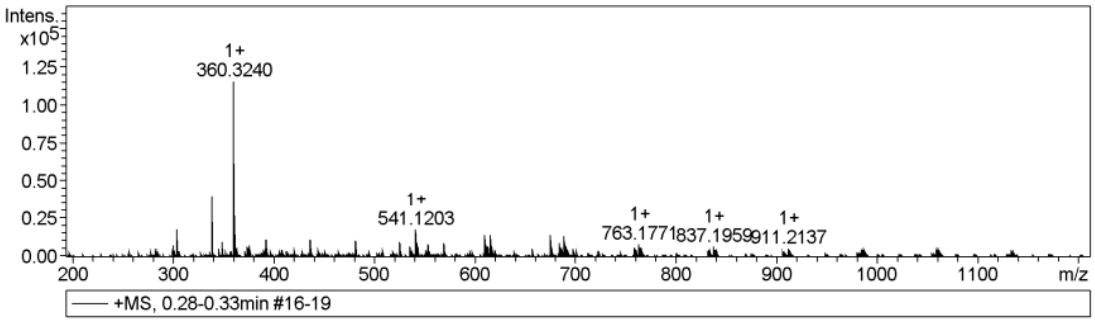

HRMS (ESI, m/z): [M]+ calcd for $C_{50}H_{32}Br_4Na$, 970.9121; found, 970.9130.

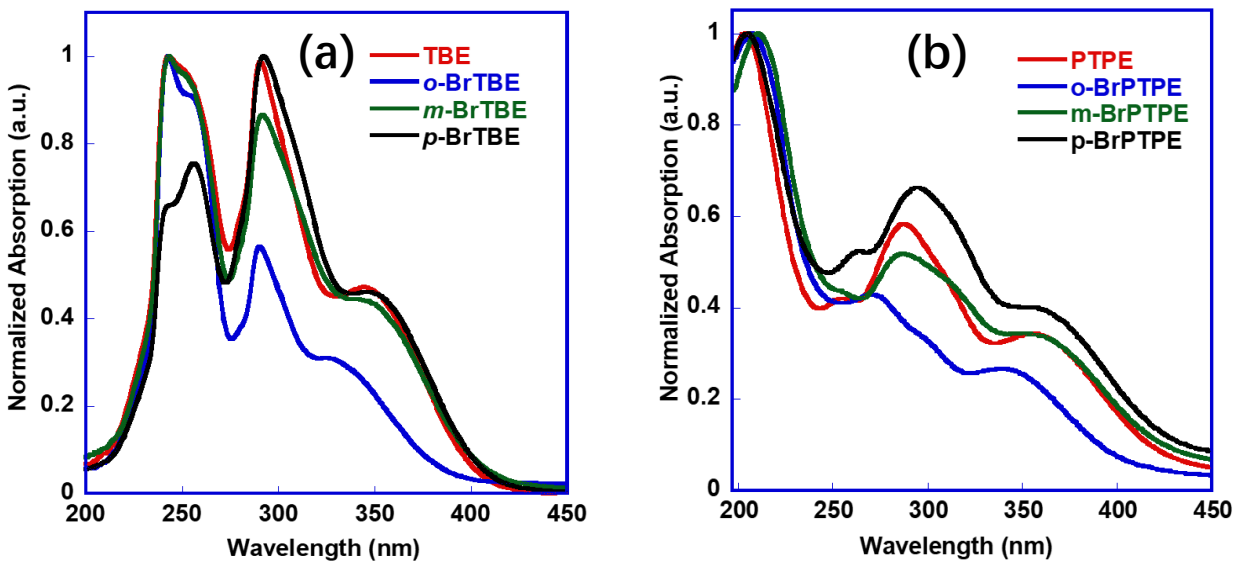

Figure S1. (a) UV-visible spectra of TBE deriatives in the dilute THF solution. Concentration: ~10 μM. (b) UV-visible spectra of TBE deriatives in the film.

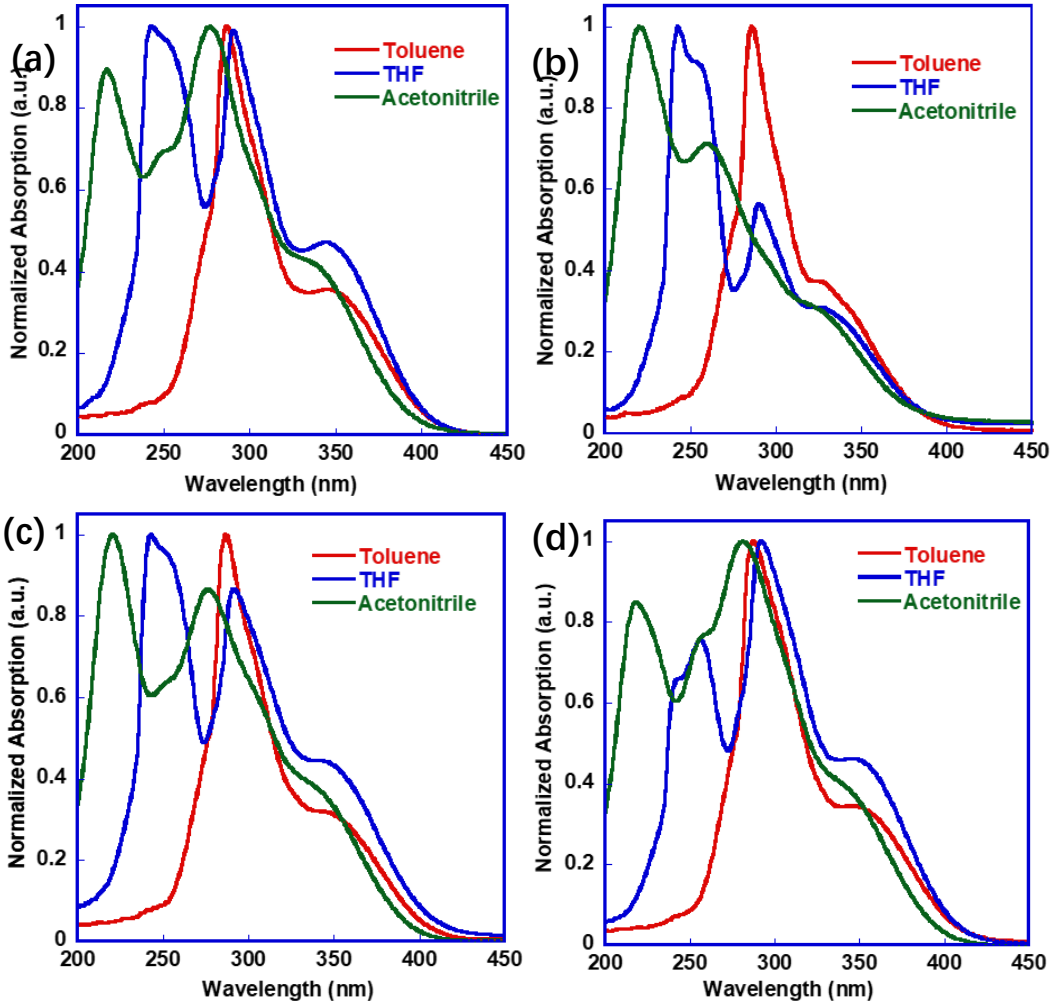

Figure S2. UV-visible spectra of TBE deriatives in different solvents.

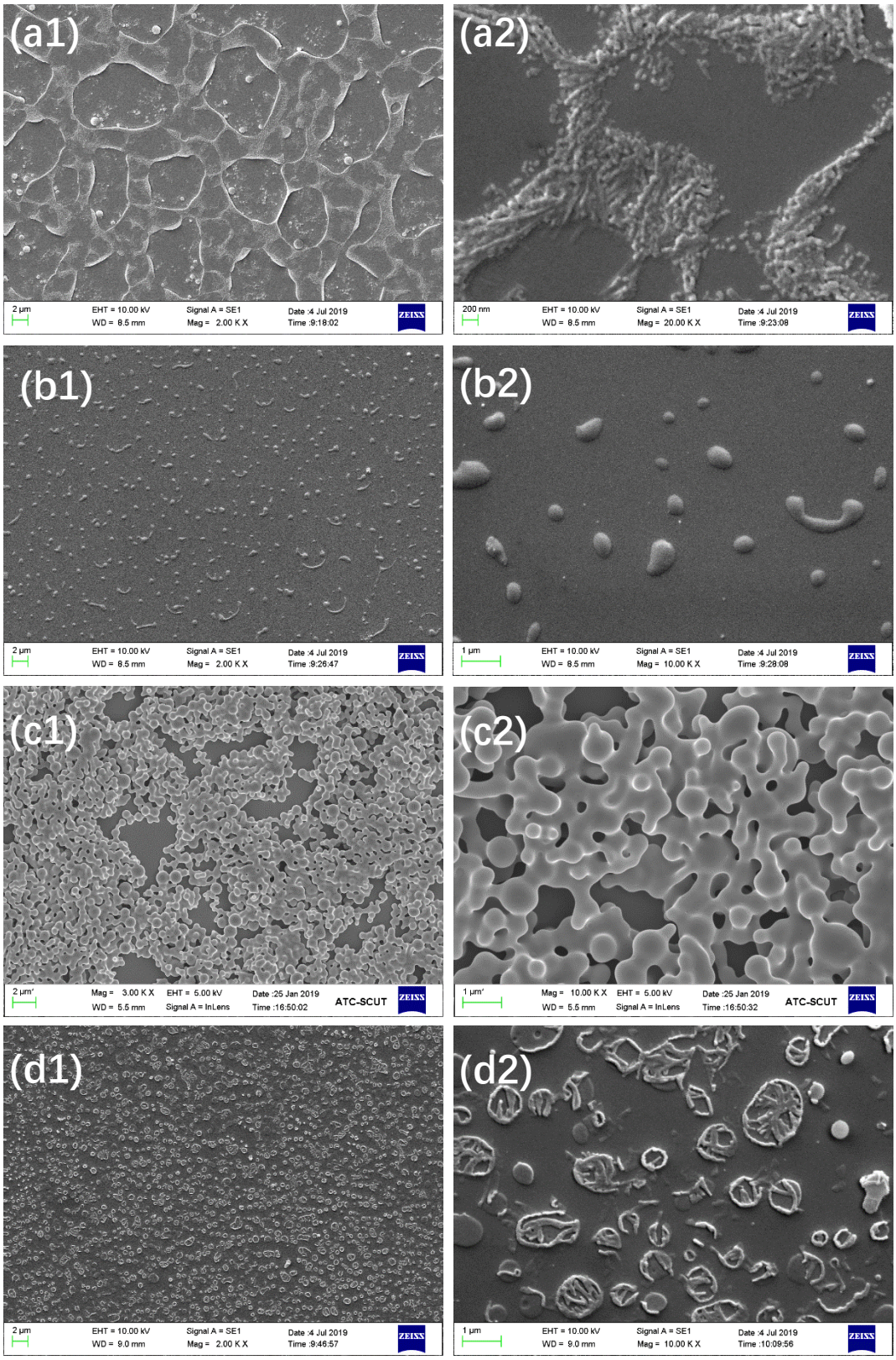

Figure S3. SEM images showing the film morphology of (a) TBE, (b) *o*-BrTBE, (c) *m*-BrTBE, and (d) *p*-BrTBE. (a1-d1) low magnification SEM images; (a2-d2) high magnification SEM images.

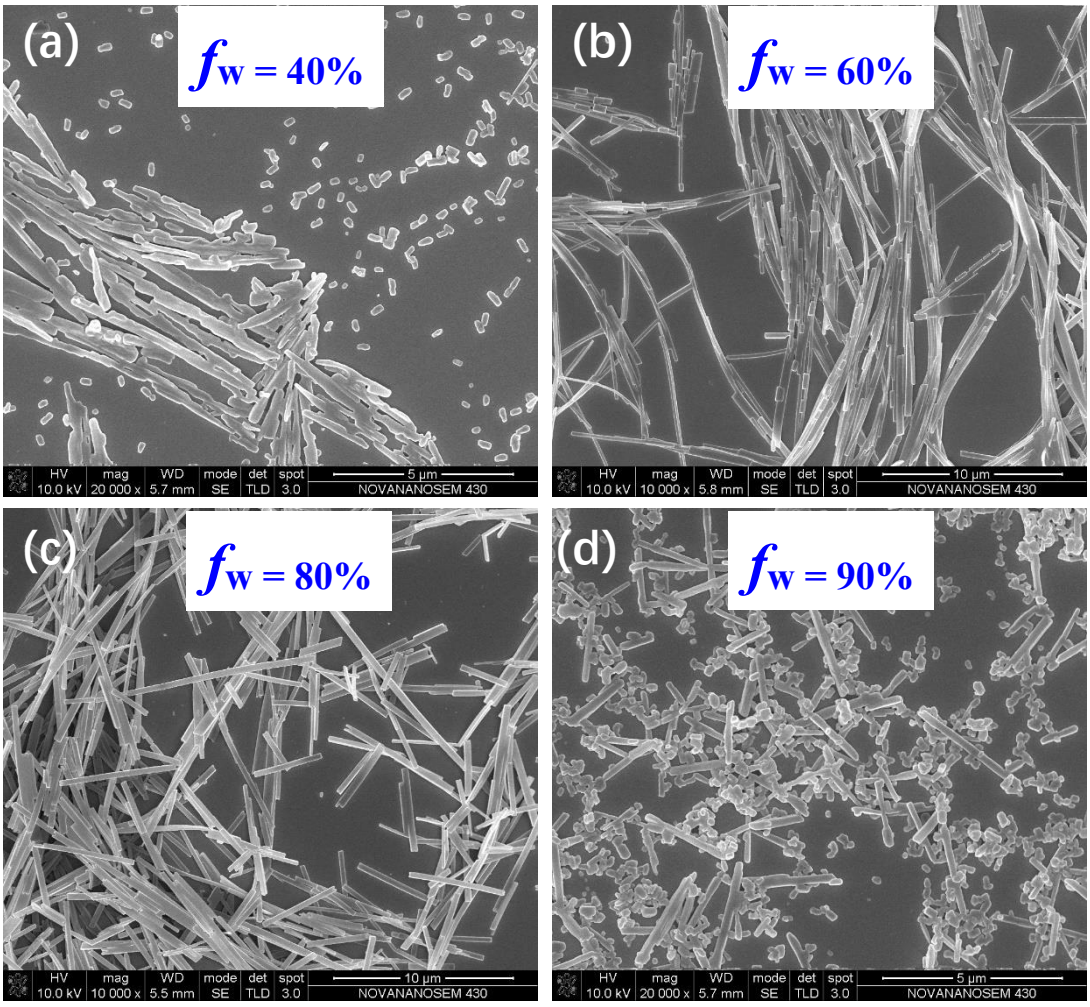

Figure S4. SEM images for the morphology of TBE aggregations in THF-water mixtures (10.0 μmol L^{-1}) with different f_w. (a) 40 %, (b) 60%, (c) 80%, (d) 90%.

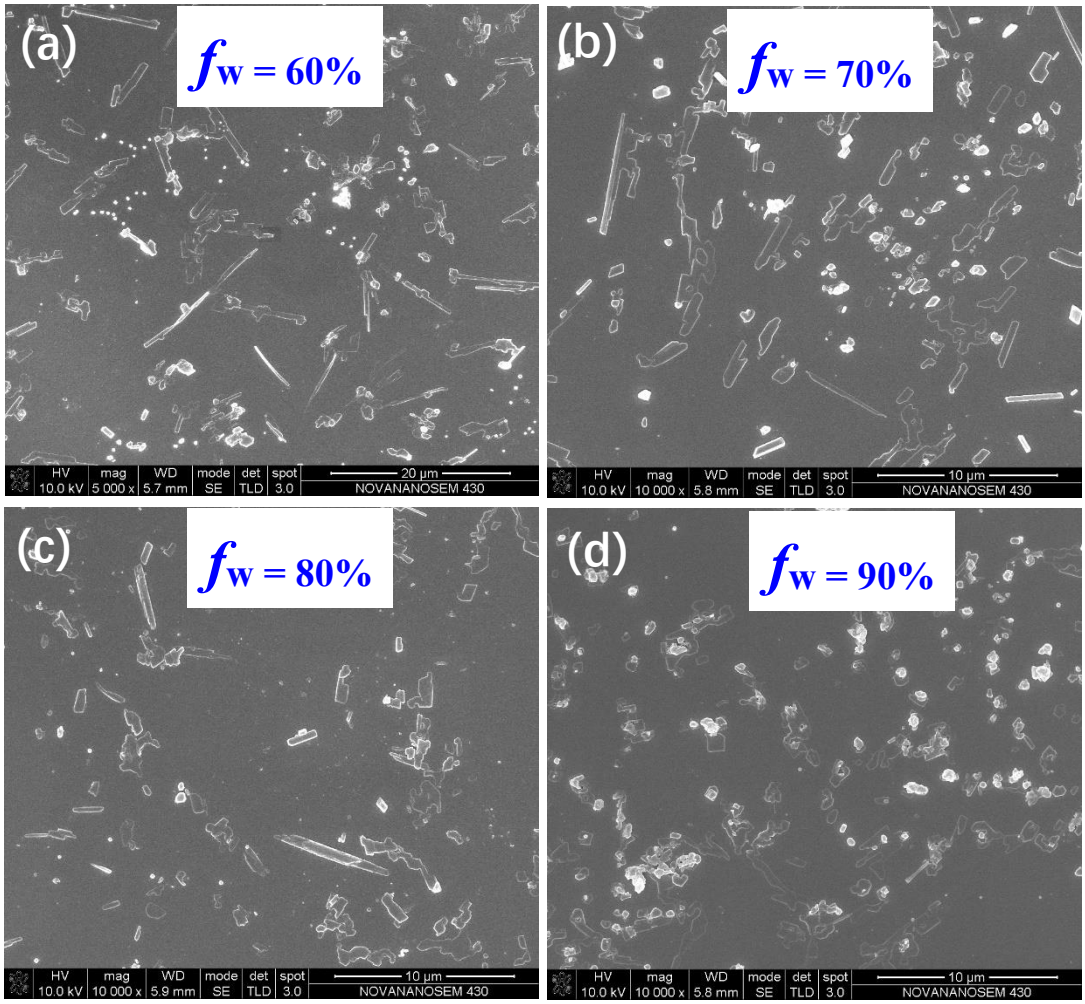

Figure S5. SEM images for the morphology of *o*-BrTBE aggregations in THF-water mixtures (10.0 μmol L^{-1}) with different f_w. (a) 60 %, (b) 70%, (c) 80%, (d) 90%.

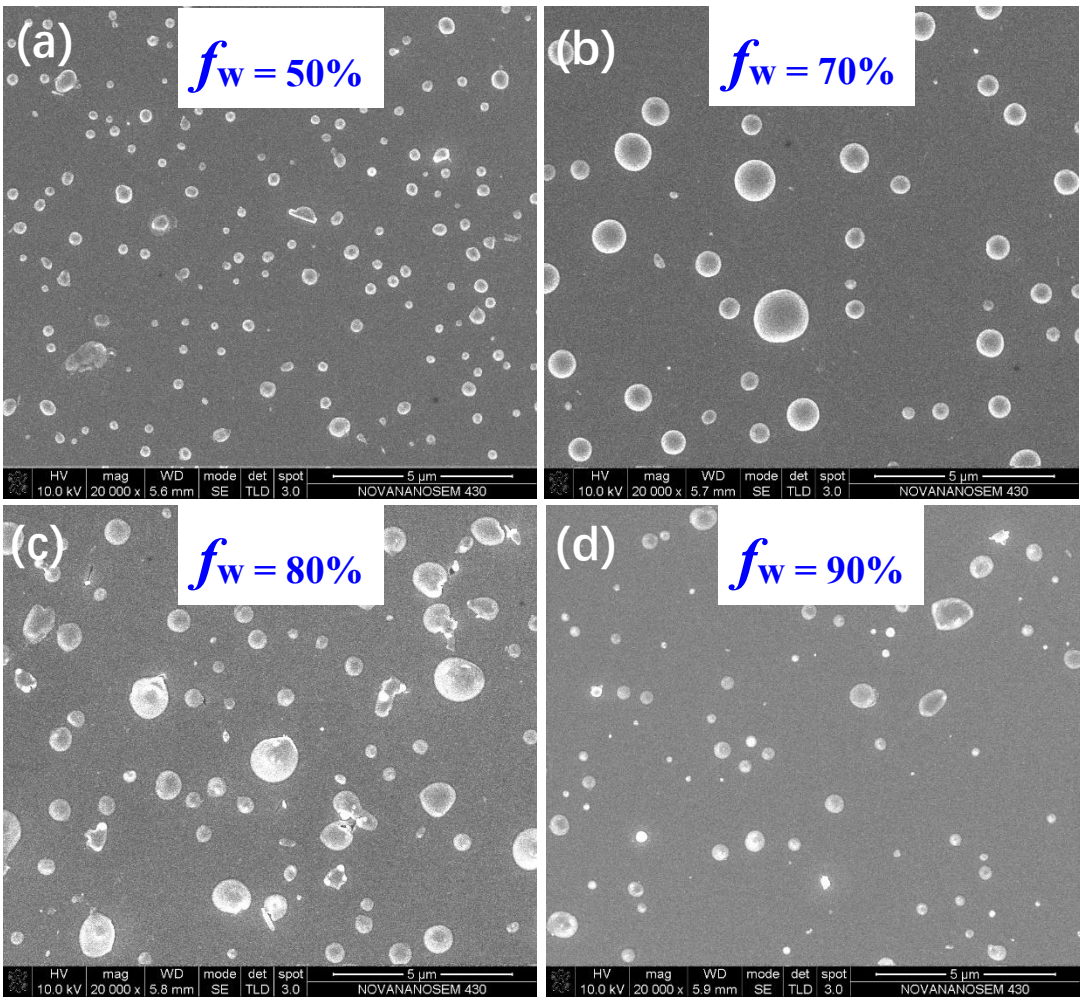

Figure S6. SEM images for the morphology of *m*-BrTBE aggregations in THF-water mixtures (10.0 μmol L^{-1}) with different f_w. (a) 50 %, (b) 70%, (c) 80%, (d) 90%.

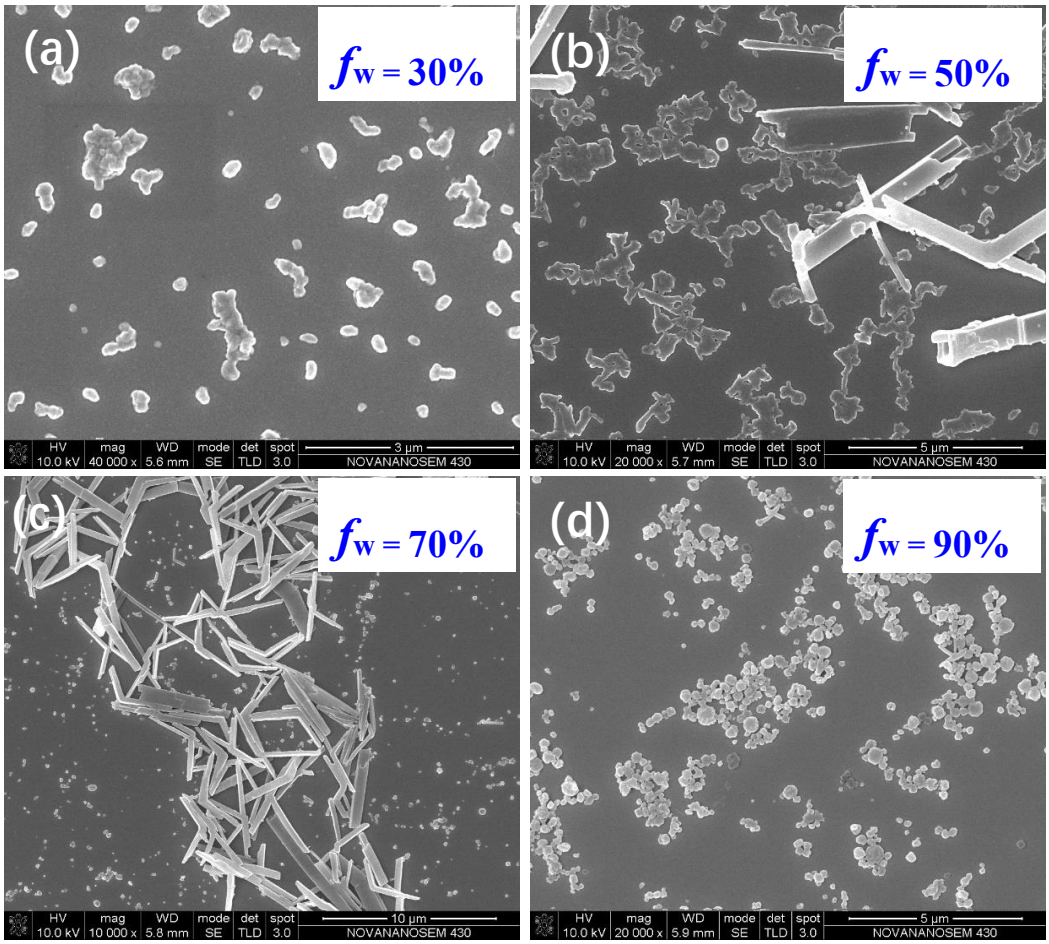

Figure S7. SEM images for the morphology of *p*-BrTBE aggregations in THF-water mixtures (10.0 μmol L^{-1}) with different f_w. (a) 30 %, (b) 50%, (c) 70%, (d) 90%.

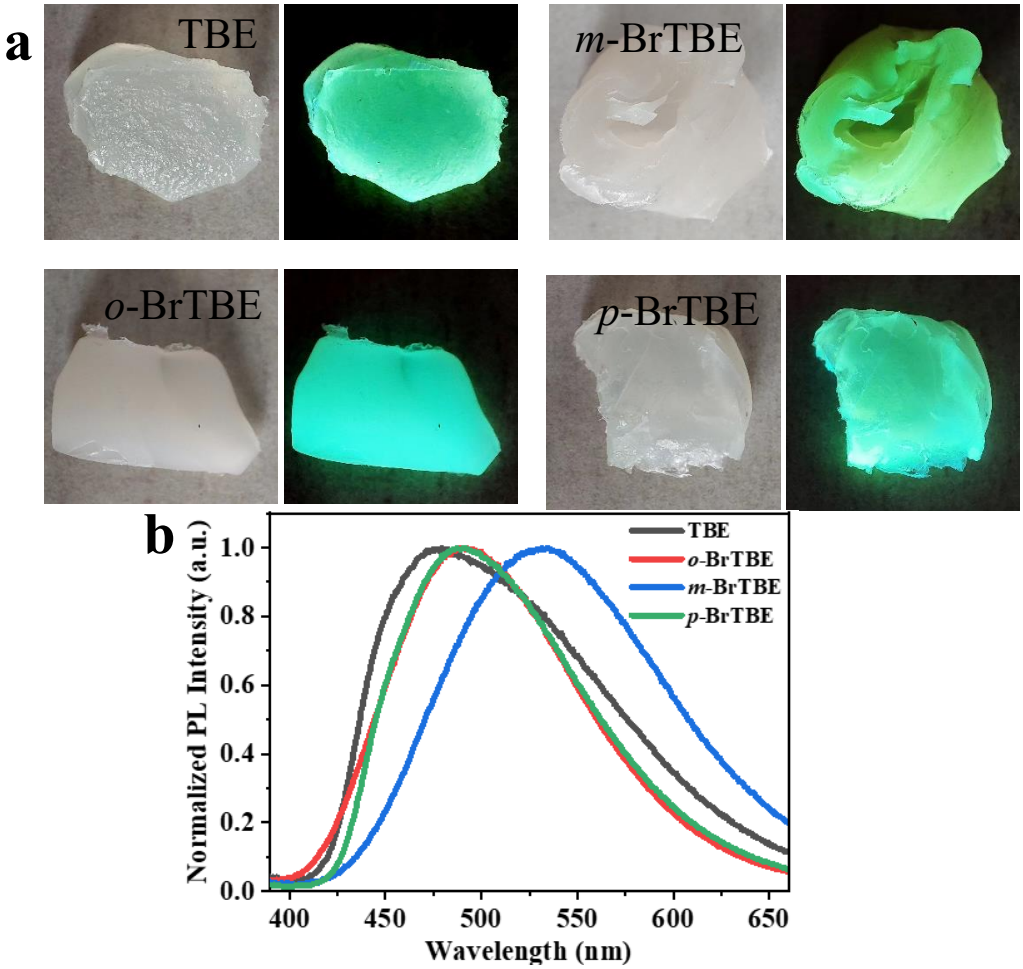

Figure S8. (a) Photo images for the TBE derivatives doped in PE with the mass ratio of 0.6% under visible light and UV-irradiation. (b) Corresponding normalized fluorescence spectra of the samples.

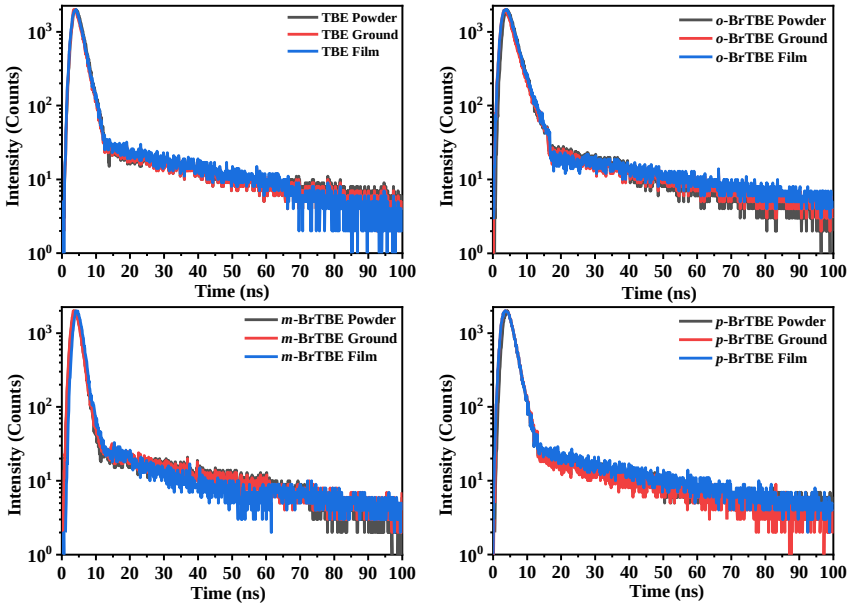

Figure S9. Time-resolved photoluminescence spectra of TBE derivatives.

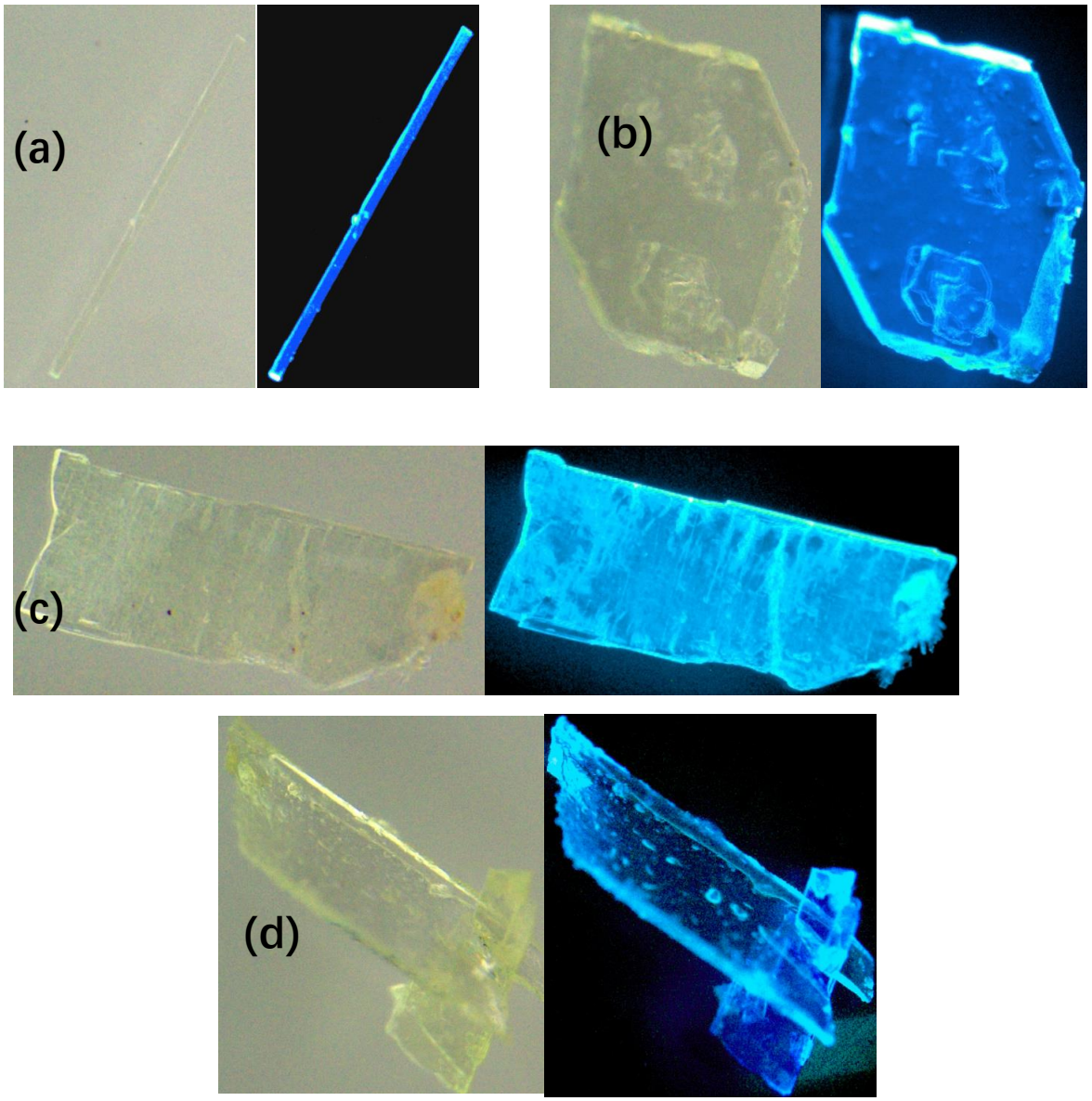

Figure S10. Photo images of crystals under visible light and under 365 nm UV irradiation. (a) , (b) *o*-BrTBE, (c) *m*-BrTBE, and (d) *p*-BrTBE.

Table S1. Summary of Crystal Data of TBE Derivatives

Parameters	TBE	*o*-BrTBE	*m*-BrTBE	*p*-BrTBE
Empirical formula	$C_{50}H_{36}$	$C_{50}H_{32}Br_4$	$C_{50}H_{32}Br_4$	$C_{50}H_{32}Br_4$
Formula weight [g mol^{-1}]	636.79	952.59	952.39	952.39
Crystal system	Triclinic	Triclinic	Triclinic	Triclinic
Space group	$P\bar{1}$	$P\bar{1}$	$P\bar{1}$	$P\bar{1}$
a [Å]	10.6929(2)	10.8896(2)	11.1418(3)	10.5007(2)
b [Å]	12.0268(2)	16.4344(3)	13.3885(2)	14.1713(3)
c [Å]	14.5008(2)	24.9108(4)	13.7139(4)	16.1575(4)
α [°]	100.6080(10)	95.290(2)	85.617(2)	71.393(2)
β [°]	104.2550(10)	101.814(2)	72.732(3)	77.081(2)
γ [°]	94.1050(10)	103.211(2)	79.248(2)	75.587(2)
Volume [$Å^3$]	1763.08(5)	4202.78(14)	1918.74(9)	2179.59(9)
Z	2	4	2	2
Density, calculated [g cm^{-3}]	1.199	1.505	1.648	1.451
Temperature [K]	149.99(10)	150.00(10)	150.00(10)	150.00(10)
Reflections collected	17040	42286	18645	22287
Independent reflections	6781	14712	6729	8403
Parameters	451	1067	489	532
R_{int}	0.0216	0.0381	0.0260	0.0262
$R_1[I > 2\sigma(I)]$	0.0382	0.0589	0.0592	0.0316
$wR_2[I > 2\sigma(I)]$	0.0959	0.1679	0.1471	0.0826
Goodness-of-fit on F^2	1.043	1.069	1.053	1.067

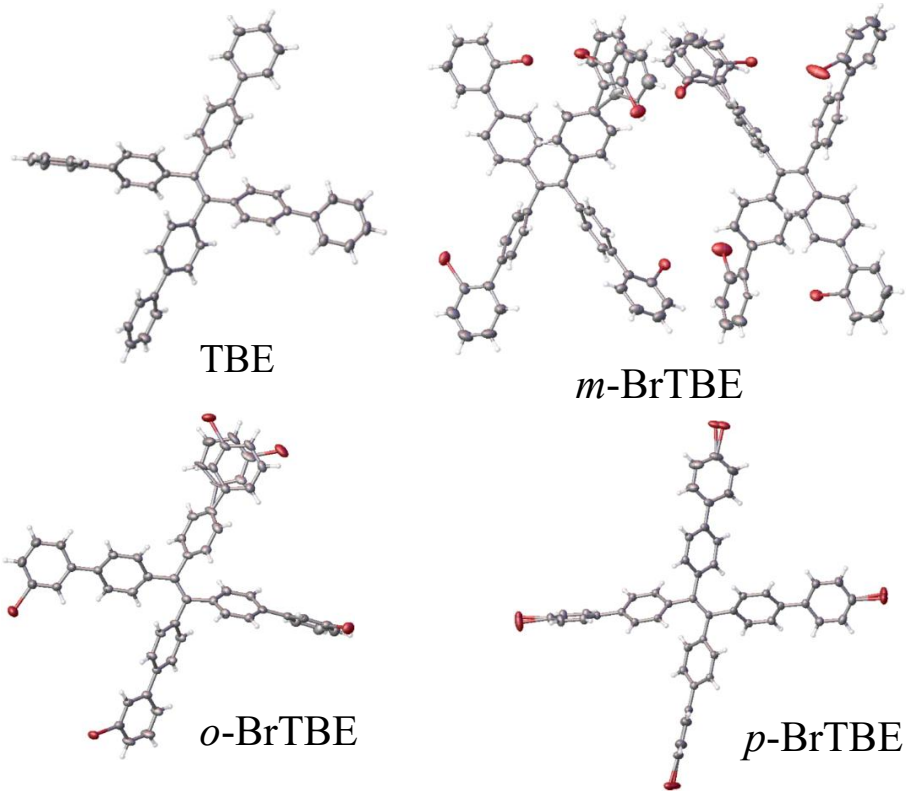

Figure S11. Molecular conformation in the crystal lattices. C (grey), H (white), Br (red).

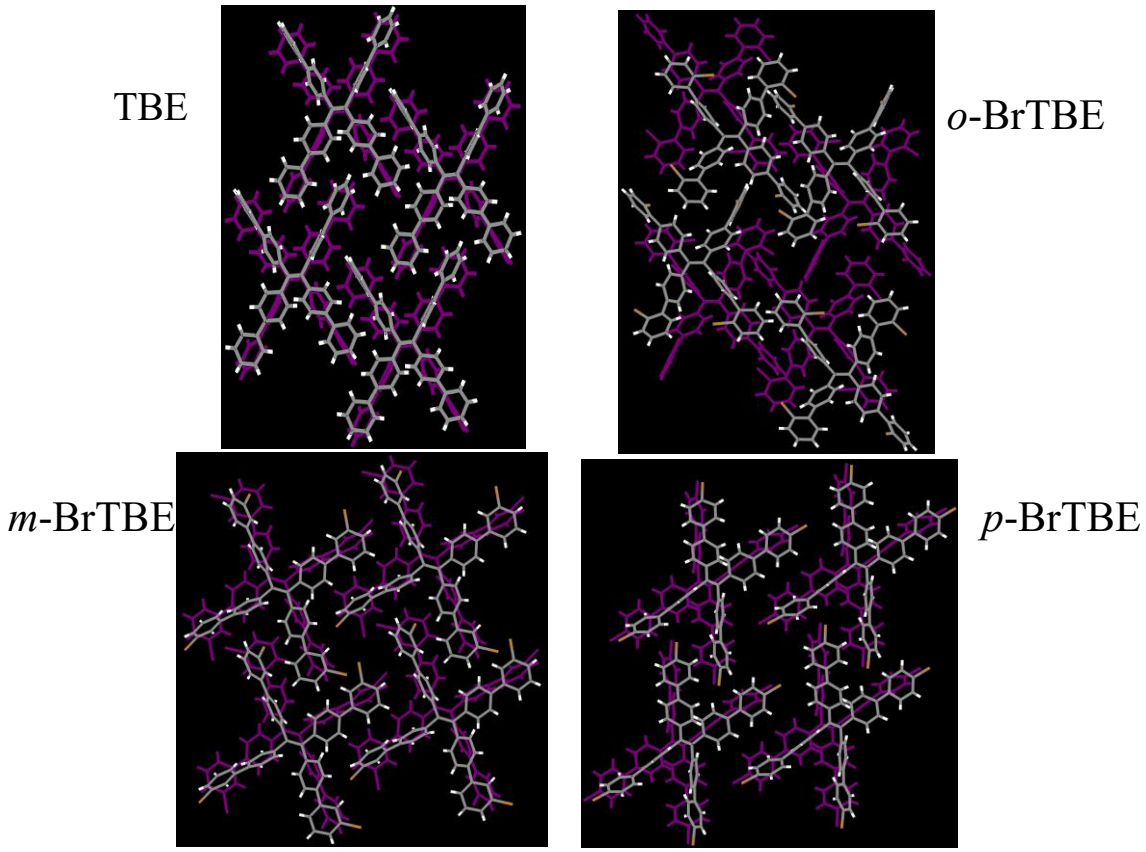

Figure S12. Two planes of TBE derivatives along *a*-axis showing different orientations in neighboring layers.

Table S2. Intermolecular interactions of eight molecules in the crystals as shown in Figure S10.

	van der Waals interaction(kJ/mol)	Coulomb interaction (kJ/mol)	Total intermolecular interaction (kJ/mol)
TBE	–864.793	–2005.77	–2870.563
o-BrTBE	–681.709	–1048.91	–1730.619
m-BrTBE	–1156.98	–1451.45	–2608.430
p-BrTBE	–961.027	–3362.59	–4323.617

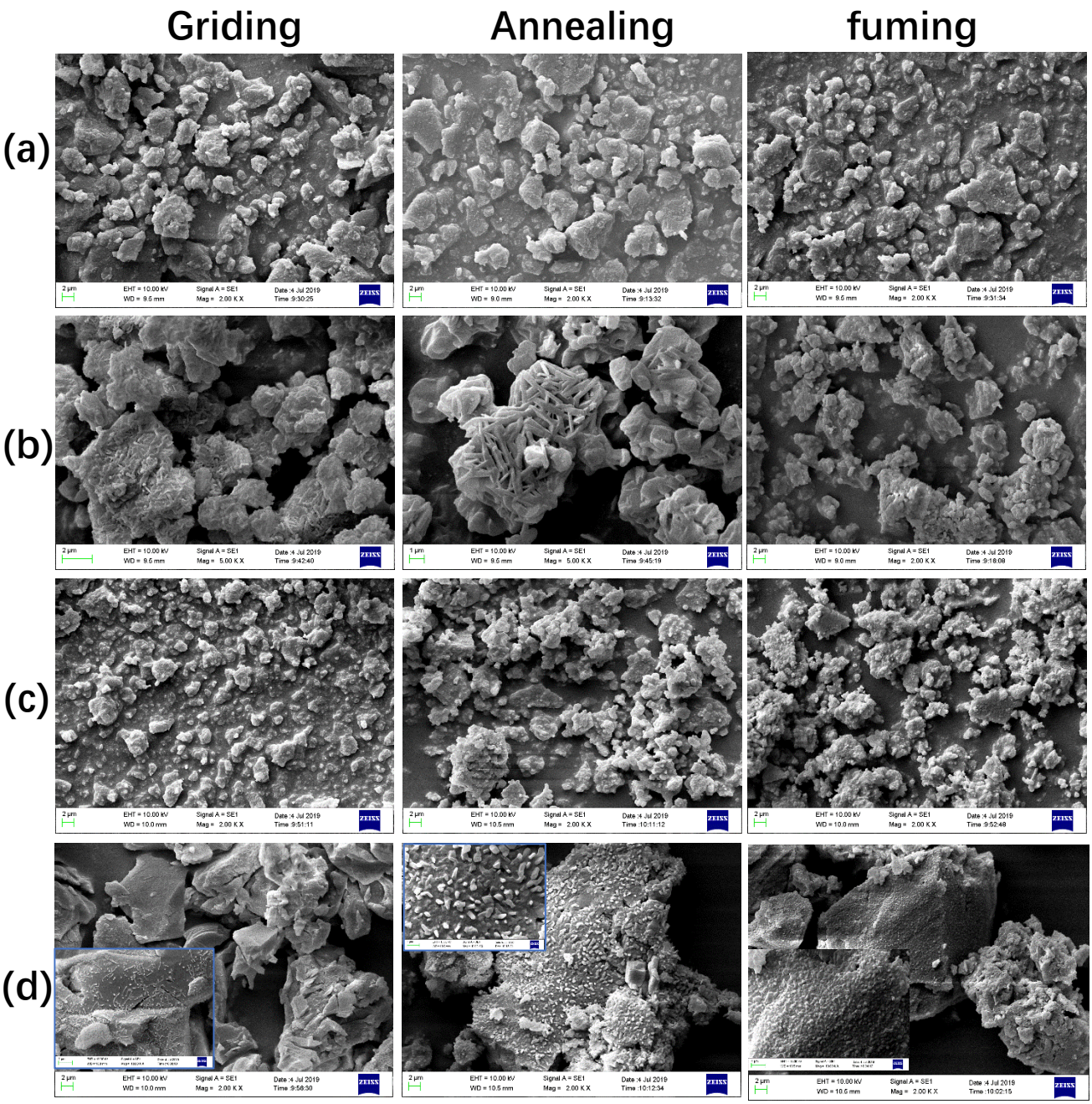

Figure S13. SEM images showing the morphology of (a) TBE, (b) *o*-BrTBE, (c) *m*-BrTBE, and (d) *p*-BrTBE powders upon griding, annealing, and fuming.